

S-matrix approach to quantum gases in the unitary limit I: the two-dimensional case

Pye-Ton How and André LeClair

Newman Laboratory, Cornell University, Ithaca, NY

Abstract

In three spatial dimensions, in the unitary limit of a non-relativistic quantum Bose or Fermi gas, the scattering length diverges. This occurs at a renormalization group fixed point, thus these systems present interesting examples of interacting scale-invariant models with dynamical exponent $z = 2$. We study this problem in two and three spatial dimensions using the S-matrix based approach to the thermodynamics we recently developed. It is well suited to the unitary limit where the S-matrix $S = -1$, since it allows an expansion in the inverse coupling. We define a meaningful scale-invariant, unitary limit in two spatial dimensions, where again the scattering length diverges. In the two-dimensional case, the integral equation for the pseudo-energy becomes transcendently algebraic, and we can easily compute the various universal scaling functions as a function of μ/T , such as the energy per particle. The ratio of the shear viscosity to the entropy density η/s is above the conjectured lower bound of $\hbar/4\pi k_B$ for all cases except attractive bosons. For attractive 2-component fermions, $\eta/s \geq 6.07 \hbar/4\pi k_B$, whereas for attractive bosons $\eta/s \geq 0.4 \hbar/4\pi k_B$.

I. INTRODUCTION

In three spatial dimensions, in the unitary limit of a quantum Bose or Fermi gas with point-like interactions, the scattering length diverges. “Unitary” here refers to the limit on the cross section imposed by unitarity. These systems provide intriguing examples of interacting, scaling invariant theories with dynamical exponent $z = 2$, i.e. non-relativistic. The infinite scattering length occurs at a fixed point of the renormalization group in the zero temperature theory, thus the models are quantum critical. The only energy scales in the problem are the temperature and chemical potential, and thermodynamic properties are expected to reveal universal behavior. They can be realized experimentally by tuning the scattering length to $\pm\infty$ using a Feshbach resonance. (See for instance [1, 2] and references therein.) They are also thought to occur at the surface of neutron stars.

The systems have attracted much theoretical interest, and remain challenging problems due to the lack of small parameter for a perturbative expansion, such as $n^{1/d}a$ or $n^{1/d}r$ where a is the scattering length, and r the range of the 2-body potential. Early works were done by Leggett and Nozières and Schmitt-Rink[3, 4]. The universal scaling behavior was studied in [5, 6]. In 3 dimensions, this is the physics of the BCS/BEC crossover: since the fixed point occurs for an attractive coupling, the fermions may form a bosonic bound state which can subsequently undergo BEC. This cross-over was studied analytically in [7] by considering a model of 2-component fermions coupled to the bosonic bound state. Monte-Carlo studies were performed in [8, 11–13]. The models can be studied in spatial dimension $2 < d < 4$ [9, 10] and an epsilon expansion carried out[14, 15]. There has also been some attempts to apply the AdS/CFT correspondence to these non-relativistic systems[16–19].

In the present work, we describe a new analytic approach to studying the unitary

limit based on our treatment of quantum gases in [20], which appears to be well suited to the problem since it allows an expansion in the inverse coupling. Let us motivate this approach as follows. In one spatial dimension, the fixed point occurs for repulsive interactions. The model is integrable[21] and its thermodynamics determined exactly by the so-called thermodynamic Bethe ansatz (TBA)[22]. In the TBA, the free energy is expressed in terms of a pseudo-energy which is a solution to an integral equation with a kernel related to the logarithm of the S-matrix. In the unitary limit the coupling goes to ∞ and the S-matrix $S = -1$. The TBA is then identical to a free gas of fermionic particles. The formalism developed in [20] was modeled after the TBA: the free energy is expressed as a sum of diagrams where the vertices represent matrix elements of the logarithm of the (zero temperature) S-matrix. However since generally the N-body S-matrix does not factorize into 2-body scattering, the series cannot be summed exactly as in the TBA. Nevertheless, a consistent resummation of an infinite number of diagrams involving only 2-body scattering, the so-called foam diagrams, can serve as a useful approximation if the gas is not too dense. The result of summing these diagrams leads to an integral equation for a pseudo-energy, as in the TBA; in fact in 1 spatial dimension the TBA is recovered to lowest order in the kernel. Since the formalism is based on the S-matrix, it can be very useful for studying the unitary limit where $S = -1$.

In this paper we present the main formulas for the 3-dimensional case, however we mainly analyze the 2-dimensional case; analysis of the 3d case will be published separately[23]. Phase transitions in two-dimensional Fermi gases were studied in e.g. [25]. The fixed point separating the BEC and BCS regimes goes to zero coupling when $d = 2$, thus it is not obvious whether a unitary limit exists at strong coupling. As we will argue, there is a scale-invariant limit at infinite coupling $g = \pm\infty$ where the S-matrix $S = -1$. This is a meaningful unitary limit at very low ($g = -\infty$) or very high ($g = +\infty$) energy, although it does not correspond to a fixed point in the

usual sense of a zero of the beta function. The scattering length indeed diverges in this limit. The possibility of this kind of unitary limit in two dimensions has not been considered before in the literature.

In the next section we describe the unitary limit in 1,2 and 3 dimensions and its relation to the renormalization group. In section III, we define the interesting scaling functions for the free energy and single-particle energies by normalizing with respect to free theories. In section IV we describe the unitary limit of the formalism in [20] in both two and three dimensions, where the integral equation becomes scale invariant. The $d = 2$ case is especially simple since the kernel reduces to a constant and the integral equation becomes algebraic. Analysis of these equations in $2d$ is carried out for both infinitely repulsive or attractive fermions and bosons in sections V-VIII. The extension of our formalism to multiple species of possibly mixed bosonic and fermionic particles is considered in section IX.

Kovtun et. al. conjectured that there is a universal lower bound to the ratio of the shear viscosity to the entropy density,

$$\eta/s \geq \frac{\hbar}{4\pi k_B} \quad (1)$$

where k_B is Boltzmann's constant[24]. This was based on the AdS/CFT correspondence for *relativistic* theories in 3 spatial dimensions, and the bound is saturated for certain supersymmetric gauge theories. Counterexamples to the η/s bound were suggested to be non-relativistic[24], however no known fluid violates the bound. It is thus interesting to study this ratio for non-relativistic theories, and in particular for $2d$ theories where no conjecture have been put forward. It has also been suggested that the gases in the unitary limit may represent the most perfect fluid, i.e. with the lowest value of η/s . For the spacetimes considered thus far for a non-relativistic AdS/CFT correspondence in 2d, the result found is that η/s is exactly $1/4\pi$ [18, 19]. We analyze η/s for the attractive fermionic case as a function of μ/T

in section VI. If one disregards unphysical, potentially metastable regions, one finds $\eta/s \geq 6.07 \hbar/4\pi k_B$. The other cases of repulsive bosons or fermions also satisfy the bound. However the attractive boson is below it: $\eta/s \geq 0.4 \hbar/4\pi k_B$.

II. RENORMALIZATION GROUP AND THE UNITARY LIMIT

The models considered in this paper are the simplest models of non-relativistic bosons and fermions with quartic interactions. The bosonic model is defined by the action for a complex scalar field ϕ .

$$S = \int d^d \mathbf{x} dt \left(i\phi^\dagger \partial_t \phi - \frac{|\vec{\nabla} \phi|^2}{2m} - \frac{g}{4} (\phi^\dagger \phi)^2 \right) \quad (2)$$

(Throughout this paper, d refers to the number of spatial dimensions). For fermions, due to the fermionic statistics, one needs at least a 2-component field $\psi_{\uparrow, \downarrow}$:

$$S = \int d^d \mathbf{x} dt \left(\sum_{\alpha=\uparrow, \downarrow} i\psi_\alpha^\dagger \partial_t \psi_\alpha - \frac{|\vec{\nabla} \psi_\alpha|^2}{2m} - \frac{g}{2} \psi_\uparrow^\dagger \psi_\uparrow \psi_\downarrow^\dagger \psi_\downarrow \right) \quad (3)$$

In both cases, positive g corresponds to repulsive interactions.

The bosonic theory only has a $U(1)$ symmetry. The fermionic theory on the other hand has the much larger $SO(5)$ symmetry. This is evident from the work[26] which considered a relativistic version, since the same arguments apply to a non-relativistic kinetic term. This is also clear from the work[15] which considered an N -component version with $Sp(2N)$ symmetry, and noting that $Sp(4) = SO(5)$.

The free versions of the above theories have a scale invariance with dynamical exponent $z = 2$, i.e. are invariant under

$$t \rightarrow \Lambda^{-2} t, \quad \mathbf{x} \rightarrow \Lambda^{-1} \mathbf{x}$$

At a renormalization group fixed point, i.e. quantum critical point, the model is expected to have the same scale invariance. It is natural to define scaling dimensions

$\dim[X]$ in units of inverse length or wave-vector \mathbf{k} , i.e. $\dim[\mathbf{k}] = 1$, $\dim[\mathbf{x}] = -1$, and $\dim[t] = -2$. Requiring the action to have zero scaling dimension gives $\dim[\phi] = \dim[\psi] = d/2$ and $\dim[g] = 2 - d$. The interaction is thus relevant for $d < 2$.

A. 3d case

The renormalization group behavior can be inferred from the coupling constant dependence of the S-matrix, or equivalently the kernels in section IV. For completeness we compute the beta function for arbitrary d in Appendix A using conventional methods. Consider first a single boson in $d = 3$ dimensions. The kernel in eq. (45) depends on the renormalized coupling g_R given in eq. (46), where Λ is a high momentum cutoff. The kernel G is related to the logarithm of the 2-body S-matrix as in eq. (41), and from this we can deduce the S-matrix function:

$$S(|\mathbf{k} - \mathbf{k}'|) = \frac{16\pi/mg_R - i|\mathbf{k} - \mathbf{k}'|}{16\pi/mg_R + i|\mathbf{k} - \mathbf{k}'|} \quad (4)$$

Galilean invariance, for equal mass particles, implies S is only a function of the relative momenta \mathbf{k}, \mathbf{k}' of the two in-coming particles. Unitarity of the S-matrix amounts to $S^*S = 1$. Defining $g = \hat{g}\Lambda^{2-d}$, and requiring g_R to be independent of Λ gives the beta-function:

$$\frac{d\hat{g}}{d\ell} = -\hat{g} - \frac{m}{4\pi^2}\hat{g}^2 \quad (5)$$

where $\ell = -\log \Lambda$ is the logarithm of a length scale. The above result agrees with the calculation in Appendix A. With the normalization of g in the fermionic case as given in (3), the resulting beta function is the same as above.

As discussed in [9, 15], the beta-function in d dimensions (see Appendix A) has the following implications. See Figure 1. For $d < 2$, there is an infra-red stable fixed point at the positive value

$$\hat{g}_* = (2 - d)\pi^{d/2}\Gamma(d/2)2^d/m \quad (6)$$

corresponding to repulsive interactions. When $d = 1$, this fixed point is approached from $g = \pm\infty$ when the cutoff Λ is infinite. In the limit of $g \rightarrow \pm\infty$ the S-matrix, as given in eq. (44) becomes $S = -1$, which is the unitary limit. In the 1-dimensional thermodynamic Bethe ansatz, the thermodynamics is simply that of a free, one-component, fermionic gas, even though the original particle was a boson.

For $d > 2$, there is an *ultra-violet* stable fixed point at the *negative* coupling \hat{g}_* , i.e. an attractive interaction. A bosonic gas with attractive interactions can be unstable. However for a fermionic gas, the attractive interaction can be balanced by the Fermi pressure, and the gas can be stable against collapse.

We now describe the implications of the above fixed point on the scattering length. Consider a single boson. A straightforward calculation of the differential cross section in d spatial dimensions gives

$$\frac{d\sigma}{d\Omega} = \frac{m^2 k^{d-3}}{4(2\pi)^{d-1}} |\mathcal{M}(k)|^2 \quad (7)$$

where $\mathcal{M}(|\mathbf{k} - \mathbf{k}'|)$ is the scattering amplitude. In the above formula k is the momentum of one of the particles in the center of mass frame, i.e. $2k = |\mathbf{k} - \mathbf{k}'|$. The \mathcal{M} are an important ingredient of the kernels of the integral equations in section IV, and were computed to all orders in [20] for instance. In $d = 3$, we equate $\sigma = \pi a^2$. This gives

$$a(k) = \frac{m}{2\pi} \frac{g_R}{\sqrt{1 + (mg_R k / 8\pi)^2}} \quad (8)$$

where g_R is the renormalized coupling (46). If $a(k)$ is measured at very small momentum transfer $|\mathbf{k} - \mathbf{k}'| \approx 0$, this leads to the definition of the scattering length

$$a = \frac{mg_R}{2\pi} = \frac{mg}{2\pi(1 + mg\Lambda/4\pi^2)} \quad (9)$$

where Λ is the ultra-violet cutoff. In order for a to diverge, g must be negative. In fact, at precisely the fixed point $g_* = \hat{g}_*/\Lambda$, $a \rightarrow \pm\infty$, depending on from which side

g_* is approached. When $g = g_*^-$, i.e. just less than g_* , then $a \rightarrow \infty$, whereas when $g = g_*^+$, $a \rightarrow -\infty$. The case $g_R = -\infty$ is on the BCS side of the crossover, whereas $g_R = +\infty$ is on the BEC side. See Figure 1.

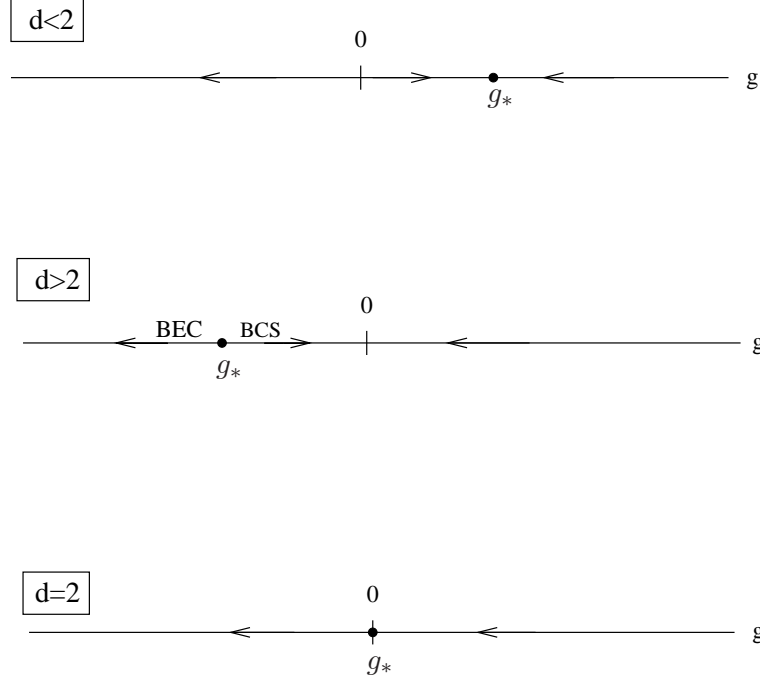


FIG. 1: Renormalization group flows; arrows indicate the flow to low energy.

The S-matrix (4) has a pole at $k = 16\pi i/mg_R$. Since physical bound states correspond to poles at $\text{Im}(k) > 0$, the bound state exists only on the BEC side of the critical point, with energy

$$E_{\text{bound-state}} = -\frac{128\pi^2}{m^3 g_R^2} \quad (10)$$

In the BEC to BCS crossover from $1/a = 0^+$ to $1/a = 1/0^-$ the binding energy goes to zero and the bound state disappears. Nevertheless, the crossover is expected to be smooth, if on the BEC side one includes the bound state in the thermodynamics.

B. 2d case

The $d = 2$ case is somewhat more subtle due to the marginality of the coupling g . The fixed point $\hat{g}_* = 0$ and the RG flows are depicted in Figure 1. The fixed point at $\hat{g}_* = 0$ is just the free field theory, thus there is no analog of the BEC/BCS cross-over. One can nevertheless formally define the unitary limit as $S = -1$, as in $1d$ and $3d$. In this subsection we explore this possibility and interpret it using the renormalization group. As we'll see, this limit occurs at $g = \pm\infty$, and the scattering length diverges.

First begin with the beta-function in 2d, eq. (110):

$$\frac{dg}{d\log\Lambda} = \frac{mg^2}{4\pi} \quad (11)$$

Let $g = g_0$ at some arbitrary scale Λ_0 . Integrating the beta function one finds:

$$g(\Lambda) = \frac{g_0}{1 - \frac{mg_0}{4\pi} \log(\Lambda/\Lambda_0)} \quad (12)$$

Note that g diverges at the scale:

$$\Lambda_* = \Lambda_0 e^{4\pi/mg_0} \quad (13)$$

This is the familiar Landau pole. Whereas in for example the relativistic ϕ^4 theory in $d = 3$ where the Landau pole is unphysical due to higher order corrections, here the beta function (11) is exact[15], thus this divergence is physical. There are two cases to consider:

Attractive case: If g_0 is negative, $\Lambda_* < \Lambda_0$, and thus $g = -\infty$ occurs in the infra-red.

Repulsive case: If g_0 is positive, $\Lambda_* > \Lambda_0$, and $g = +\infty$ occurs in the ultra-violet.

Both cases are consistent with the flows depicted in Figure 1.

In fact, the scale $\Lambda_* = \Lambda e^{4\pi/mg}$ is an RG invariant:

$$\frac{d\Lambda_*}{d\log\Lambda} = 0 \quad (14)$$

and is the natural coupling constant in this problem that physical quantities are expressed in terms of. The S-matrix can be inferred from the kernel in eq. (48):

$$S(|\mathbf{k}|) = \frac{4\pi/mg + \log(2\Lambda/|\mathbf{k}|) - i\pi/2}{4\pi/mg + \log(2\Lambda/|\mathbf{k}|) + i\pi/2} \quad (15)$$

$$= \frac{\log(2\Lambda_*/|\mathbf{k}|) - i\pi/2}{\log(2\Lambda_*/|\mathbf{k}|) + i\pi/2} \quad (16)$$

where $|\mathbf{k}| = |\mathbf{k}_1 - \mathbf{k}_2|$ is the relative momentum of the two incoming particles. Near the fixed point $g = 0^-$, $\Lambda_* = 0$ ($\Lambda_* = \infty$) and the S-matrix $S = 1$, consistent with the free theory. The same applies to the other side of the fixed point $g = 0^+$ where $\Lambda_* = \infty$. On the other hand, consider the low energy limit of the attractive case where $g = -\infty$. Here $\Lambda_* = \Lambda$, and this scale is effectively an infra-red cutoff. Thus at low energies $|\mathbf{k}_1 - \mathbf{k}_2| \approx 2\Lambda_*$ and $S = -1$. Similar arguments apply to the high energy limit of the repulsive case $g = +\infty$. It is clear that, unlike in $3d$, this definition of the unitary limit does not correspond to a renormalization group fixed point in the usual sense of a zero of the beta function and is somewhat engineered; nevertheless it defines a scale-invariant theory.

Let us turn now to the scattering length. Using the scattering amplitude \mathcal{M} computed in [20], the cross section for relative momenta $2k$ is:

$$\sigma(k) = \frac{m^2 g^2}{8k} \frac{1}{(1 + \frac{mg}{4\pi} \log(\Lambda/k))^2 + \pi^2} \quad (17)$$

$$= \frac{2\pi^2}{k} \frac{1}{\log^2(\Lambda_*/k) + 16\pi^4/m^2 g^2} \quad (18)$$

Near the scale $k = \Lambda_*$:

$$\sigma(\Lambda_*) = \frac{2}{\Lambda_*} \left(\frac{mg}{4\pi} \right)^2 \quad (19)$$

Equating σ with a scattering length a , as appropriate to $2d$, one sees that a diverges in the unitary limit $g \rightarrow \pm\infty$.

Because of the logarithmic dependence on $|\mathbf{k}_1 - \mathbf{k}_2|$, the S-matrix does not have a pole. However the denominator is zero when $|\mathbf{k}_1 - \mathbf{k}_2| = 2k = 2i\Lambda_*$, which is a remanant of the bound state pole in $3d$. The energy of this quasi-bound state is $-2\Lambda_*^2/m$. Note that this quasi-bound state disappears as $g_0 \rightarrow 0^-$, since in this limit $\Lambda_* \rightarrow 0$, and this is analagous to the situation in $3d$. We thus expect that the “attractive” case of the unitary limit should be better behaved since this bound state disappears, in contrast to the repulsive case where $\Lambda_* \rightarrow \infty$ as $g_0 \rightarrow 0^+$, and this will be born out of our subsequent analysis.

III. THERMODYNAMIC SCALING FUNCTIONS AT THE QUANTUM CRITICAL POINT

At a quantum critical point, the only length scales of the quantum gas are the thermal wavelength $\lambda_T = \sqrt{2\pi/mT}$ and the length scale $n^{1/d}$ set by the density n . Equivalently, one can express physical properties in terms of the only two energy scales, the temperature T and the chemical potential μ , since the density is a function of T, μ .

In order to fix normalizations in a meaningful way, it is useful to consider the simplest theories with $z = 2$ scale invariance: free, non-relativistic bosons and fermions. We set $k_B = \hbar = 1$, except in a few select formulas. The free energy density is given by the well-known expression for each particle:

$$\mathcal{F} = \frac{s}{\beta} \int \frac{d^d \mathbf{k}}{(2\pi)^d} \log (1 - s e^{-\beta(\omega_{\mathbf{k}} - \mu)}) \quad (20)$$

where $\beta = 1/T$, $\omega_{\mathbf{k}} = \mathbf{k}^2/2m$ and $s = 1, -1$ corresponds to bosons, fermions respectively. The integrals over wave-vectors can be expressed in terms of polylogarithms

$\text{Li}_\nu(z)$, where $z = e^{\beta\mu}$ is a fugacity, using $\int d^d\mathbf{k} = 2\pi^{d/2}/\Gamma(d/2) \int dk k^{d-1}$ and the integrals

$$\begin{aligned}\int_0^\infty dx \frac{zx^{\nu-1}}{e^x - z} &= \Gamma(\nu) \text{Li}_\nu(z) \\ \int_0^\infty dx \frac{zx^{\nu-1}}{e^x + z} &= -\Gamma(\nu) \text{Li}_\nu(-z)\end{aligned}\quad (21)$$

valid for $\text{Re}(\nu) > 0$. The result, as expected, is proportional to T/λ_T^d :

$$\mathcal{F} = -sT \left(\frac{mT}{2\pi} \right)^{d/2} \text{Li}_{(d+2)/2}(sz) \quad (22)$$

There are two important limits to consider. For Bose gases near Bose-Einstein condensation, physically the interesting limit is $\mu/T \rightarrow 0$. Since $\text{Li}_\nu(1) = \zeta(\nu)$, where ζ is Riemann's zeta function, this leads us to define the scaling functions $c_d(\mu/T)$:

$$\begin{aligned}\mathcal{F} &= -\frac{\pi m T^2}{12} c_2(\mu/T) & (d=2) \\ \mathcal{F} &= -\frac{\zeta(5/2) m^{3/2} T^{5/2}}{(2\pi)^{3/2}} c_3(\mu/T) & (d=3)\end{aligned}\quad (23)$$

where we have used $\zeta(2) = \pi^2/6$. With the above normalizations, $c_d = 1$ for a single free boson when $\mu/T = 0$.

The above formulas are well-defined for fermions at zero chemical potential. Using

$$-\text{Li}_\nu(-1) = \left(1 - \frac{1}{2^{\nu-1}} \right) \zeta(\nu) \quad (24)$$

one finds as $\mu/T \rightarrow 0$:

$$c_2 = \frac{1}{2}, \quad c_3 = 1 - \frac{1}{2\sqrt{2}} \quad (\text{free fermions}) \quad (25)$$

It should be pointed out that the coefficients c_d are analogous to the Virasoro central charge for relativistic systems in $d = 1$, as discussed in [27].

The other interesting limit is $T/\mu \rightarrow 0$, i.e. $z \rightarrow \infty$ or $z \rightarrow 0$, depending on the sign of the chemical potential. Here the scaling forms are naturally based on the

zero temperature degenerate free fermion gas, where $\mu > 0$ is the Fermi energy. In fact, the function $\text{Li}_\nu(z)$ has a branch cut along the real axis from $z = 1$ to ∞ and the bosonic free energy is ill-defined at $z = \infty$, in contrast with fermions. Using the analytic continuation of the asymptotic behavior

$$-\text{Li}_\nu(-z) \approx \frac{\log^\nu(z)}{\Gamma(\nu + 1)} \quad \text{as } z \rightarrow \infty \quad (26)$$

from positive integer ν to half-integer values, we define the scaling functions b_d as follows:

$$\begin{aligned} \mathcal{F} &= -\frac{m\mu^2}{4\pi} b_2(T/\mu) & (d=2) \\ \mathcal{F} &= -\frac{2\sqrt{2}m^{3/2}\mu^{5/2}}{15\pi^2} b_3(T/\mu) & (d=3) \end{aligned} \quad (27)$$

The above normalizations are defined such that $b_d(0) = 1$ for a single free fermion. One can verify that the above $d = 3$ expression is the standard result for a zero temperature, single component, degenerate fermion gas where μ is the Fermi energy.

Other thermodynamic quantities follow from the free energy. The pressure $p = -\mathcal{F}$. The density is $n = -\partial\mathcal{F}/\partial\mu$ and the entropy density is $s = -\partial\mathcal{F}/\partial T$. Using the scaling form in eq. (27), one obtains for $d = 3$:

$$\begin{aligned} n &= \frac{2\sqrt{2}}{15\pi^2} (m\mu)^{3/2} \left(\frac{5}{2} b_3 - \frac{T}{\mu} b'_3 \right) \\ s &= \frac{2\sqrt{2}}{15\pi^2} (m\mu)^{3/2} b'_3(T/\mu) \end{aligned} \quad (28)$$

where b' is the derivative with respect to its argument T/μ . (Henceforth, g' will always refer to the derivative of the function g with respect to its argument μ/T or T/μ as defined above.) The analogous formulas in 2 dimensions are:

$$\begin{aligned} n &= \frac{m\mu}{4\pi} \left(2b_2 - \frac{T}{\mu} b'_2 \right) \\ s &= \frac{m\mu}{4\pi} b'_2 \end{aligned} \quad (29)$$

The energy density ϵ follows from the relation $\epsilon = Ts + \mu n + \mathcal{F}$:

$$\epsilon = -\frac{d}{2}\mathcal{F} \quad (30)$$

It is interesting to note that the above result, which in terms of the pressure is simply $\epsilon = pd/2$, is a consequence of the mechanics of *free* gases. This shows that this relation continues to hold for interacting gases at a quantum critical point, as pointed out by Ho[5].

Also of interest is the energy per particle $\epsilon_1 = \epsilon/n$:

$$\epsilon_1 = -\frac{d}{2}\frac{\mathcal{F}}{n} \quad (31)$$

Consider first the limit $T/\mu \rightarrow 0$, with μ positive. In this limit, if b is a smooth function of T/μ as $T/\mu \rightarrow 0^+$, then the b' terms in the density vanish and one simply obtains

$$\lim_{T/\mu \rightarrow 0^+} \epsilon_1 = \frac{d}{d+2}\mu \quad (32)$$

which is the same result as for a free gas, where for fermions μ is equal to the Fermi energy ϵ_F . The above formula is usually not appropriate to the $T \rightarrow 0$ limit when μ is negative. For the interacting gas $\mu \neq \epsilon_F$, so this leads us to define the scaling functions ξ :

$$\xi_d(T/\mu) = \frac{d+2}{d} \frac{\epsilon_1}{\epsilon_F} \quad (33)$$

As $T/\mu \rightarrow 0^+$, the functions ξ_d should become universal constants, and for free fermions $\xi_d(0^+) = 1$. The Fermi energy ϵ_F can be defined based on its relation to density in the zero temperature free fermion gas. For bosons, one can formally use the same definition. For $d = 2$, $\epsilon_F = 2\pi n/m$, whereas for $d = 3$, $\epsilon_F = (3\pi^2 n/\sqrt{2})^{2/3}/m$. This leads to the definitions:

$$\begin{aligned} \xi_2 &= \left(\frac{m\mu}{2\pi n}\right)^2 b_2(T/\mu) \\ \xi_3 &= \left(\frac{\sqrt{2}}{3\pi^2 n}\right)^{5/3} (m\mu)^{5/2} b_3(T/\mu) \end{aligned} \quad (34)$$

Next consider the energy per particle in the limit $\mu/T \rightarrow 0$. Here it is more appropriate to use the form in eq. (23), which gives

$$\epsilon_1 = \frac{d c_d}{2 c'_d} T \quad (35)$$

The expression for ϵ_1 for free fermions in the limit $\mu/T \rightarrow 0$ in $d = 3$ leads us now to define $\tilde{\xi}$:

$$\epsilon_1 = \frac{3}{2} \left(\frac{2\sqrt{2}-1}{2\sqrt{2}-2} \right) \frac{\zeta(5/2)}{\zeta(3/2)} T \tilde{\xi}_3(\mu/T) \quad (36)$$

With this normalization, for free fermions, as $\mu/T \rightarrow 0$, $\tilde{\xi}_3 = 1$.

In two dimensions, ϵ_1 goes to zero for free bosons as $\mu/T \rightarrow 0$ since it is proportional to $1/\zeta(1)$. However ϵ_1 is finite for fermions in this limit. Using $\lim_{d \rightarrow 2} (2^{d/2} - 2)\zeta(d/2) = 2 \log 2$, we define

$$\epsilon_1 = \frac{\pi^2 T}{12 \log 2} \tilde{\xi}_2(\mu/T) \quad (d = 2) \quad (37)$$

With the above normalization, $\tilde{\xi}_2(0) = 1$ for free fermions.

Henceforth we drop the subscripts 2, 3 indicating the spatial dimension on the functions c_2, c_3 etc., since in the sequel we will carry out the analysis of the $d = 2$ case only.

IV. THERMODYNAMICS FROM THE S-MATRIX IN THE UNITARY LIMIT FOR D=2,3

In the formalism developed in [20], the contributions to the free energy can be expressed as vacuum diagrams where the vertices are matrix elements of the logarithm of the S-matrix, and the lines are the filling fractions. There are vertices with $2N$ lines representing N -body scattering for any N . The main result obtained in [20], and reviewed below, is the formula for the free energy density in a self-consistent

resummation of the 2-body scattering “foam diagrams”. The 2-body scattering can be computed to all orders in the coupling in a standard zero-temperature calculation. Clearly this result is still an approximation in that higher N-body scattering, and 2-body scattering contributions not of the foam diagram type, are neglected. Nevertheless, this approximation is expected to be valid when the gas is sufficiently dilute.

The main ingredients of the formalism are as follows. Define the filling fractions as a function of a pseudo-energy $\varepsilon(\mathbf{k})$

$$f(\mathbf{k}) = \frac{1}{e^{\beta\varepsilon(\mathbf{k})} - s} \quad (38)$$

which determine the density:

$$n = \int \frac{d^d\mathbf{k}}{(2\pi)^d} \frac{1}{e^{\beta\varepsilon(\mathbf{k})} - s} \quad (39)$$

The consistent summation of 2-body scattering leads to an integral equation for the pseudo-energy $\varepsilon(\mathbf{k})$:

$$\varepsilon(\mathbf{k}) = \omega_{\mathbf{k}} - \mu - \frac{1}{\beta} \log \left(1 + \beta \int (d\mathbf{k}') G(\mathbf{k}, \mathbf{k}') \frac{e^{\beta(\varepsilon(\mathbf{k}') - \omega_{\mathbf{k}'} + \mu)}}{e^{\beta\varepsilon(\mathbf{k}')} - s} \right) \quad (40)$$

The kernel G in this equation is related to the logarithm of the 2-body S-matrix \hat{S} as follows:

$$2\pi\delta \left(E - \frac{1}{2m}(\mathbf{k}^2 + \mathbf{k}'^2) \right) V G(\mathbf{k}, \mathbf{k}') \equiv -i \langle \mathbf{k}, \mathbf{k}' | \log \hat{S}(E) | \mathbf{k}, \mathbf{k}' \rangle. \quad (41)$$

where V is the spatial volume and $(d\mathbf{k}) = d^d\mathbf{k}/(2\pi)^d$. The kernel has the following structure:

$$G = -\frac{i}{\mathcal{I}} \log(1 + i\mathcal{I}\mathcal{M}) \quad (42)$$

where \mathcal{M} is the scattering amplitude and \mathcal{I} represents the available phase space for two-body scattering. The argument of the log can be identified as the S-matrix

function. Finally, the free energy density then takes the simple form:

$$\mathcal{F} = -\frac{1}{\beta} \int (d\mathbf{k}) \left(s \log(1 + sf) - \frac{1}{2} \left(\frac{f - f_0}{1 + sf_0} \right) \right)$$

where f_0 is the filling fraction of the free theory:

$$f_0(\mathbf{k}) = \frac{1}{e^{\beta(\omega_{\mathbf{k}} - \mu)} - s} \quad (43)$$

Consider first the 1-dimensional bosonic case. The model is integrable, which implies that the N-body S-matrix factorizes into 2-body S-matrices, and the exact free energy is given by the thermodynamic Bethe ansatz[22]. The 2-body S-matrix is

$$S(k - k') = \frac{k - k' - ig/4}{k - k' + ig/4} \quad (44)$$

In the unitary limit $g \rightarrow \pm\infty$, $S = -1$, and the thermodynamic Bethe ansatz reduces to that of a free gas of fermionic particles.

In 3 spatial dimensions the exact kernel for a single component boson is the following[20]:

$$\begin{aligned} G(|\mathbf{k} - \mathbf{k}'|) &= -\frac{8\pi i}{m|\mathbf{k} - \mathbf{k}'|} \log \left(\frac{1 - \frac{img_R}{16\pi}|\mathbf{k} - \mathbf{k}'|}{1 + \frac{img_R}{16\pi}|\mathbf{k} - \mathbf{k}'|} \right) \\ &= -\frac{16\pi}{m|\mathbf{k} - \mathbf{k}'|} \arctan \left(\frac{mg_R}{16\pi}|\mathbf{k} - \mathbf{k}'| \right) \end{aligned} \quad (45)$$

where g_R is a renormalized coupling:

$$\frac{1}{g_R} = \frac{1}{g} + \frac{m\Lambda}{4\pi^2}. \quad (46)$$

with Λ an ultra-violet momentum cutoff. As in the 1-dimensional case, as discussed in section II, the unitary limit corresponds to $g_R \rightarrow \pm\infty$ where $S = -1$. Thus in the unitary limit the kernel becomes

$$G(\mathbf{k}, \mathbf{k}') = \mp \frac{8\pi^2}{m|\mathbf{k} - \mathbf{k}'|} \quad (d = 3) \quad (47)$$

where $-$, $+$ corresponds to g being just below, above g_* , where the scattering length $a = +\infty$ (BEC side) and $a = -\infty$ (BCS side) respectively. It should be kept in mind that the underlying interactions are attractive in both cases since the fixed point occurs at negative g .

In two spatial dimensions the single boson kernel obtained in [20] is

$$\begin{aligned}
G(|\mathbf{k}|) &= -\frac{4i}{m} \log \left(\frac{1 + \frac{mg}{4\pi} \left(\log \left(\frac{2\Lambda}{|\mathbf{k}|} \right) - i\pi/2 \right)}{1 + \frac{mg}{4\pi} \left(\log \left(\frac{2\Lambda}{|\mathbf{k}|} \right) + i\pi/2 \right)} \right) \\
&= -\frac{8}{m} \arctan \left(\frac{mg/8}{1 + \frac{mg}{4\pi} \log \left(\frac{2\Lambda}{|\mathbf{k}|} \right)} \right) \\
&= -\frac{8}{m} \arctan \left(\frac{2\pi}{\log(2\Lambda_*/|\mathbf{k}|)} \right)
\end{aligned} \tag{48}$$

where Λ_* is defined in eq. (13), and $|\mathbf{k}| = |\mathbf{k}_1 - \mathbf{k}_2|$ is the relative momentum. In the unitary limit $g \rightarrow \pm\infty$, the theory is at the scale Λ_* and one should consider $|\mathbf{k}_1 - \mathbf{k}_2| \approx 2\Lambda_*$. The result is that G becomes a constant in this unitary limit:

$$G(|\mathbf{k}|) = \mp \frac{4\pi}{m} \quad (d = 2) \tag{49}$$

In the attractive case, $|\mathbf{k} - \mathbf{k}'|$ approaches $2\Lambda_*$ from above as $g \rightarrow -\infty$, and thus corresponds to the $+$ sign above. The $-$ sign then corresponds to the repulsive case where $2\Lambda_*$ is approached from below.

For two-component fermions, the phase space factors \mathcal{I} in [20] are doubled, and since $G \propto 1/\mathcal{I}$, the kernels have an extra $1/2$ in the fermionic case:

$$G_{\text{fermi}} = \frac{1}{2} G_{\text{bose}} \tag{50}$$

The above unitary limit of the kernels leads to a scale-invariant integral equation for the pseudo-energy, which in turn leads to the scaling forms of the previous section. This will be described in detail for the $d = 2$ case in subsequent sections. Note

that the kernel has a well-defined expansion in $1/g$; in the sequel we only consider the above leading terms. Solving the integral equation for intermediate values of g between 0 and $\pm\infty$ and inputting the solution into the expression for the free energy should track the RG flow between $g = 0^-$ and $-\infty$, or between $g = +\infty$ and 0^+ , however we will not study this in the present work.

V. ATTRACTIVE FERMIONS IN 2 DIMENSIONS

The two-dimensional case is considerably simpler to analyze since the kernel G is a constant. In any dimension it is convenient to define:

$$\delta(\mathbf{k}) \equiv \varepsilon(\mathbf{k}) - \omega_{\mathbf{k}} + \mu; \quad y(\mathbf{k}) \equiv e^{-\beta\delta(\mathbf{k})} \quad (51)$$

The expression (43) for the free energy can be simplified to the following:

$$\mathcal{F} = -\frac{1}{\beta} \int (d\mathbf{k}) \left[-s \log(1 - se^{-\beta\varepsilon}) - \frac{1}{2} \frac{(1 - y^{-1})}{e^{\beta\varepsilon} - s} \right] \quad (52)$$

Consider first a hypothetical single component fermion. In order to have a point-like local interaction one needs at least two components, and this will be treated in section VIII. As explained there, due to the SU(2) symmetry, the two-component fermion reduces to two identical copies of the following 1-component results. Since the kernel is independent if \mathbf{k} , δ is a constant. The integral equation then becomes the transcendental algebraic equation:

$$y = 1 \mp \frac{1}{y} \log(1 + zy) \quad (53)$$

(We have used $-\text{Li}_1(-z) = \log(1 + z)$.) The $- (+)$ sign corresponds to the repulsive (attractive) case. The free energy takes the form eq. (23) where the scaling function, expressed in terms of the fugacity z , is

$$c = -\frac{6}{\pi^2} \left(\text{Li}_2(-zy) + \frac{1}{2}(1 - y^{-1}) \log(1 + zy) \right) \quad (54)$$

The scaling function b in eq. (27) is

$$b = \frac{\pi^2}{3 \log^2 z} c \quad (55)$$

and the density is

$$n = \frac{mT}{2\pi} \log(1 + zy) \quad (56)$$

The energy per particle scaling function $\tilde{\xi}$ is also expressed in terms of c :

$$\tilde{\xi} = \frac{2 \log 2}{\log(1 + zy)} c \quad (57)$$

Finally ξ takes the form:

$$\xi = \left(\frac{\log z}{\log(1 + zy)} \right)^2 b \quad (58)$$

We will mainly plot these quantities against μ/T or its inverse; these functions are implicitly functions of the more physical quantity T/T_F , where $T_F = \epsilon_F/k_B$ is the Fermi temperature. The relation with μ/T is

$$\frac{T}{T_F} = \frac{1}{\log(1 + zy)} \quad (59)$$

There exists a solution to eq. (53) for any z , i.e. for all $-\infty < \mu/T < +\infty$. The density is shown in Figure 2 and takes on all positive values and approaches ∞ as $\mu/T \rightarrow \infty$. As $T/\mu \rightarrow 0^+$, the density approaches the free field value $n = m\mu/2\pi$. However at high temperatures there is a departure from the free field value:

$$\lim_{\mu/T \rightarrow 0} n = 0.9546 \frac{mT}{2\pi} \quad (60)$$

The filling fraction f is plotted in Figure 3. The scaling function c is shown in Figure 4. One finds:

$$\lim_{\mu/T \rightarrow 0} c = 0.624816 \quad (61)$$

which is higher than the free field value $c = 1/2$. From these results, one obtains the equation of state:

$$p = 1.077 nT, \quad (\mu/T \rightarrow 0) \quad (62)$$

One needs to make sure that all regions of μ/T are physical, and not for instance metastable. In particular, the entropy must increase with temperature, otherwise the specific heat is negative. In Figure 5 we plot the entropy density s , and one sees that $\partial s/\partial T < 0$ when $\mu/T > 11.7$. One must bear in mind that our formalism, though non-perturbative in some respects, is still an approximation, and such a feature could be an artifact that disappears once the corrections are incorporated. Since it is beyond the scope of this work to systematically explore these corrections, we will instead try and interpret our results as they are, for this and subsequent cases. The above feature of the entropy density could signify a phase transition at $\mu/T = 11.7$, where the density and temperature are related by:

$$n = 13.1 \frac{mT}{2\pi} \quad \Longleftrightarrow \quad T_c = 0.076 T_F \quad (63)$$

where T_F is the Fermi temperature ϵ_F/k_B , where ϵ_F is defined in section III, and T_c is the critical temperature for this hypothetical phase transition. The above value is comparable to the prediction $T_c \approx 0.1 T_F$ in [25] for quasi 2d (trapped) systems. In all other regions, and for all other cases considered below, $\partial s/\partial T > 0$.

The scaling function b is shown in Figure 6. It has a well defined limit as $T/\mu \rightarrow 0$, however the limiting value depends on whether μ is positive or negative:

$$\lim_{T/\mu \rightarrow 0^-} b = 0, \quad \lim_{T/\mu \rightarrow 0^+} b = 1 \quad (64)$$

Recall $b = 1$ is the free fermion value. The discontinuity at $T/\mu = 0$ is traced to the fact that $c(\infty) \neq c(-\infty)$, and has no physical significance. Since the density approaches $m\mu/2\pi$, the equation of state is

$$p = 2\pi n^2/m, \quad (\mu/T \rightarrow \infty) \quad (65)$$

The energy per particle scaling function $\tilde{\xi}$ is shown in Figure 7. It has the limiting values:

$$\lim_{\mu/T \rightarrow 0} \tilde{\xi} = 0.907412, \quad \lim_{\mu/T \rightarrow -\infty} \tilde{\xi} = 0.842766, \quad \lim_{\mu/T \rightarrow \infty} \tilde{\xi} = \infty \quad (66)$$

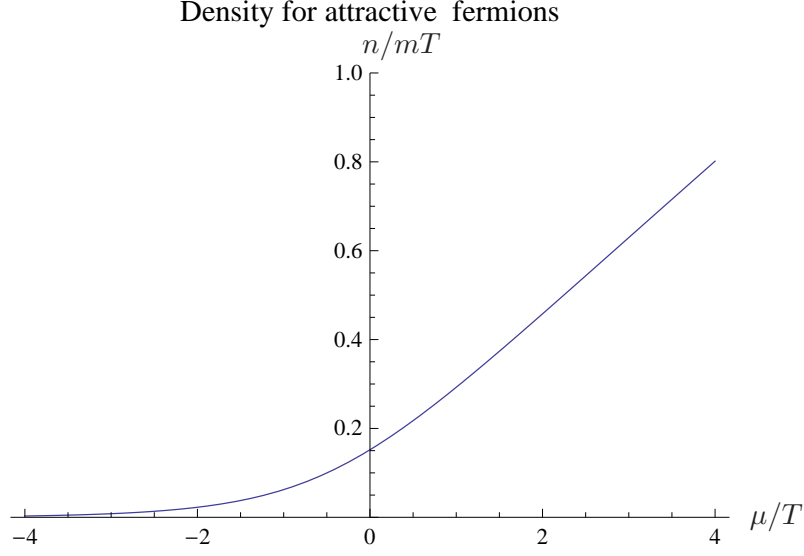


FIG. 2: Density of the attractive fermionic case as a function of μ/T .

The above value for $\tilde{\xi}$ as $\mu/T \rightarrow -\infty$ was determined numerically, however it turns out to equal $12 \log 2/\pi^2$. Equation (37) then shows that the energy per particle $\epsilon_1 = T$, which simply means that in the limit $\mu/T \rightarrow -\infty$ the gas is effectively classical. This feature will be encountered in other cases below.

The single particle energy scaling function ξ has the behaviour shown in Figure 8. It has the limiting behavior

$$\lim_{T/\mu \rightarrow 0^+} \xi = 1, \quad \lim_{T/\mu \rightarrow \pm\infty} \xi = 2.25593 \quad (67)$$

The value $\xi(0) = 1$ is consistent with the arguments in [10]. It diverges as $T/\mu \rightarrow 0^-$ due to the vanishing density at $\mu/T \rightarrow -\infty$.

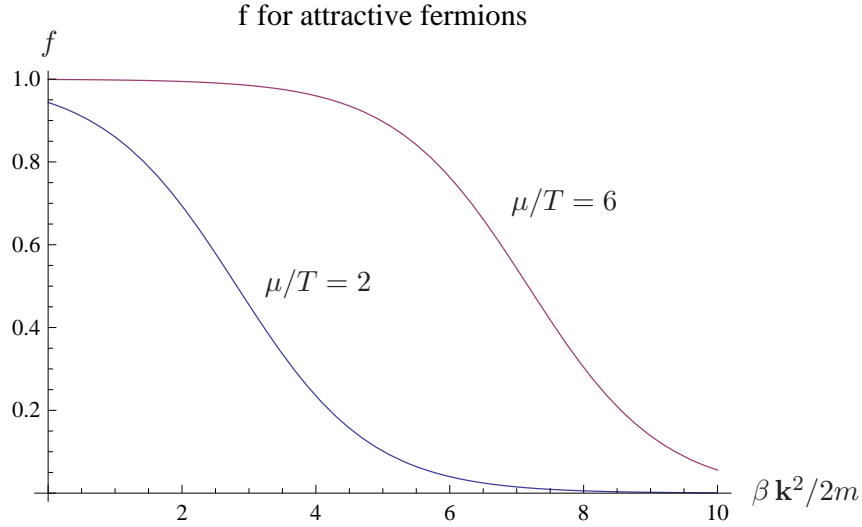


FIG. 3: Filling fraction f for attractive fermions at two different values of μ/T .

VI. RATIO OF SHEAR VISCOSITY TO ENTROPY DENSITY

The ratio of the shear viscosity η to the entropy density s has units of \hbar/k_B in any dimension. A lower bound was conjectured for 3d relativistic systems[24]:

$$\frac{\eta}{s} \geq \frac{\hbar}{4\pi k_B} \quad (68)$$

based on the AdS/CFT correspondence. The bound is saturated in certain strongly coupled supersymmetric gauge theories. It is therefore interesting to study this ratio for non-relativistic, strongly interacting systems, in 3 and lower dimensions, since it is unknown whether there really is a lower bound. This ratio was studied for 3d unitary Fermi gases in [29–32]. The attractive fermion case is the most interesting and well-behaved case in our formalism, as will be evident in the subsequent sections, so we study the issue in this case first.

Consider first a gas with a single species of particle of mass m . For a non-

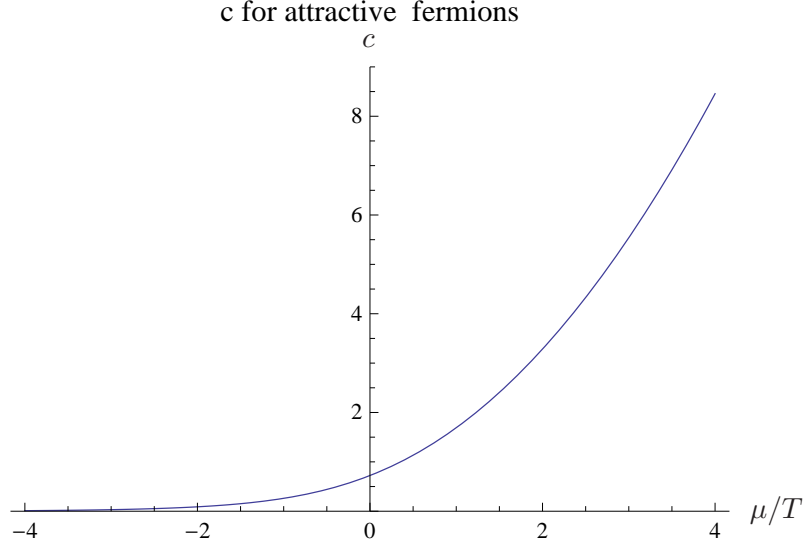


FIG. 4: The scaling function c for attractive fermions as a function of μ/T .

relativistic system in 2 spatial dimensions:

$$\eta = \frac{1}{2} n \bar{v} m \ell_{\text{free}} \quad (69)$$

where \bar{v} is the average speed and ℓ_{free} the mean free path. The mean free path is $\ell_{\text{free}} = 1/(\sqrt{2}n\sigma)$ where σ is the total cross-section. The $\sqrt{2}$ comes from the ratio of the mean speed to the mean relative speed[28]. In the unitary limit, formally $S = 1 + i\mathcal{I}\mathcal{M} = -1$, which implies the scattering amplitude $\mathcal{M} = 2i/\mathcal{I}$. (See section IV.) The cross-section in eq. (7) gives $\sigma = m^2/k\mathcal{I}^2$ in 2 dimensions, where $\mathcal{I} = m/4$ [20]. Thus, in the unitary limit

$$\sigma = \frac{16}{|\mathbf{k}|} \quad (70)$$

where \mathbf{k} is a single particle momentum. This gives

$$\eta = \frac{m}{16\sqrt{2}} \left(\frac{1}{2} m \bar{v}^2 \right) \quad (71)$$

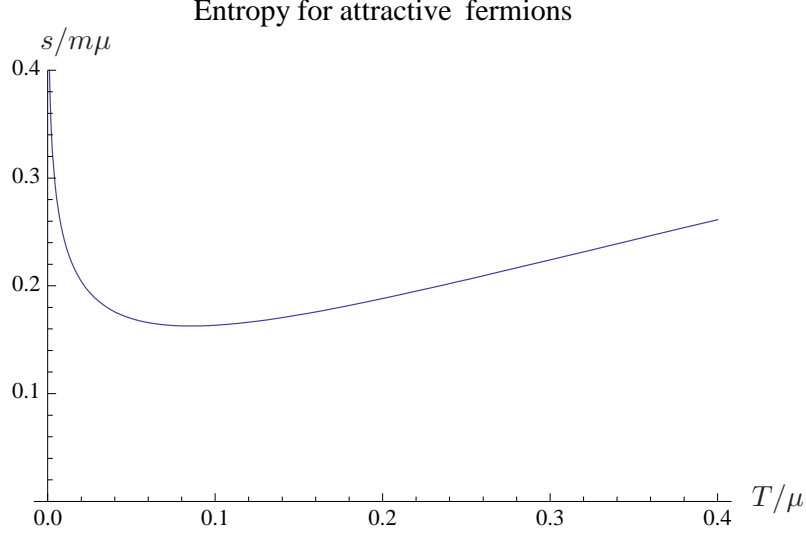


FIG. 5: The entropy density s divided by $m\mu$ for attractive fermions as a function of T/μ .

Since the pressure is determined by the average kinetic energy, and the ideal gas relation eq. (30) still holds for a unitary gas, the average kinetic energy per particle is just $\epsilon_1 = -\mathcal{F}/n$, eq. (31). Finally we obtain:

$$\frac{\eta}{s} = \frac{m}{16\sqrt{2}} \frac{\mathcal{F}}{n} \left(\frac{\partial \mathcal{F}}{\partial T} \right)^{-1} \quad (72)$$

where all the quantities in the above formula are the single component values of the last section. In terms of the scaling functions:

$$\frac{\eta}{s} = \frac{3}{4\sqrt{2}\pi} \frac{c}{c'} \frac{1}{(2c - \frac{\mu}{T}c')} = \frac{\pi}{4\sqrt{2}} \frac{b}{b'} \frac{1}{(2b - \frac{T}{\mu}b')} \quad (73)$$

For two-component fermions the available phase space \mathcal{I} is doubled. The cross-section is halved since spin up particles only scatter with spin down. Finally the entropy is doubled. This gives

$$\left(\frac{\eta}{s} \right)_{\text{fermi}} = 4 \left(\frac{\eta}{s} \right)_{\text{bose}} \quad (74)$$

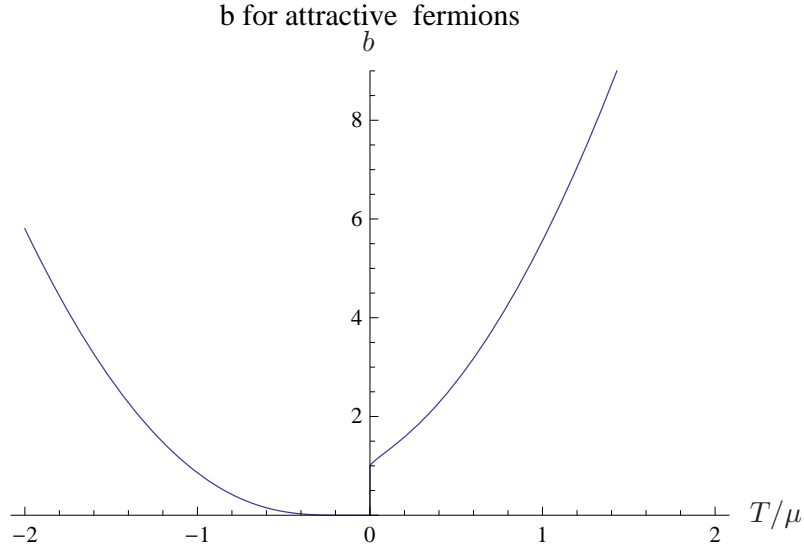


FIG. 6: The scaling function b for attractive fermions as a function of T/μ .

The above expression is easily evaluated numerically using the expressions of the last section. The result is displayed for small values of μ/T in Figure 9. In this regime, η/s is well above the conjectured bound, and comparable to the $3d$ values extracted from the experimental data[31]. We find

$$\lim_{\mu/T \rightarrow 0} \frac{\eta}{s} = 7.311 \frac{\hbar}{4\pi k_B} \quad (75)$$

This is well-below the values for common substances like water, however it is comparable to values for liquid helium, which is about 9 times the bound[24]. In the region shown:

$$\frac{\eta}{s} \geq 6.07 \frac{\hbar}{4\pi k_B} \quad (76)$$

In Figure 10 we plot η/s as a function of T/T_F , and one observes a behavior quite similar both qualitatively and quantitatively to the $3d$ data summarized in[31], where the minimal value is about 6 times the bound.

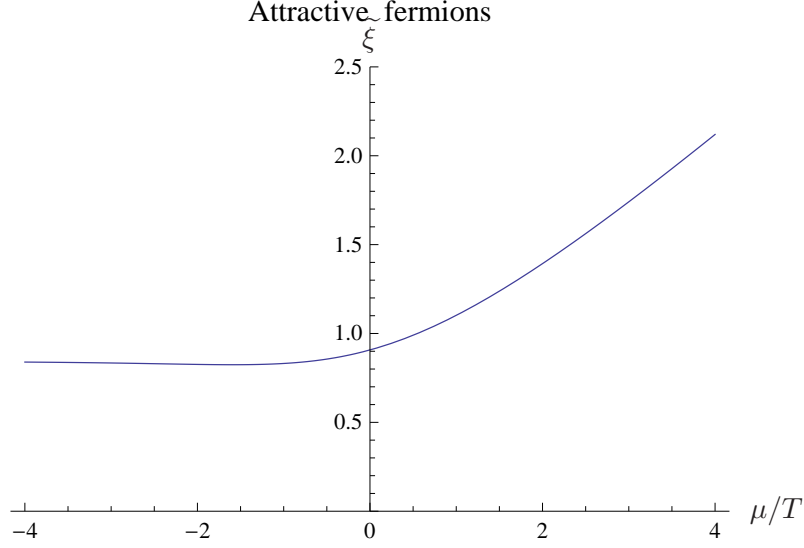


FIG. 7: The energy per particle scaling function $\tilde{\xi}$ for attractive fermions as a function of μ/T .

Recall that in the last section, it was argued that the region $\mu/T > 11.7$ is unphysical, or perhaps metastable, since the entropy increases with decreasing temperature there. Thus for the regions that are surely physical, the bound (76) holds. It is nevertheless interesting to study the viscosity in this unphysical region. In the zero temperature limit, i.e. $T/\mu \rightarrow 0^+$, η/s slowly decreases and seems to approach the bound. See Figure 11. However it eventually dips below it. See Figure 12. This behavior can be understood analytically as follows. For $x = \mu/T$ very large, the solution to the equation (53) is approximately:

$$y(x) \approx \sqrt{x} + 1/2 + (\log x - 1)/4\sqrt{x} \quad (77)$$

This leads to the asymptotic expansions:

$$\begin{aligned} c &\approx 3(x^2 + x \log x - x)/\pi^2 \\ n &\approx \frac{mT}{2\pi}(x + \log(x)/2) \end{aligned} \quad (78)$$

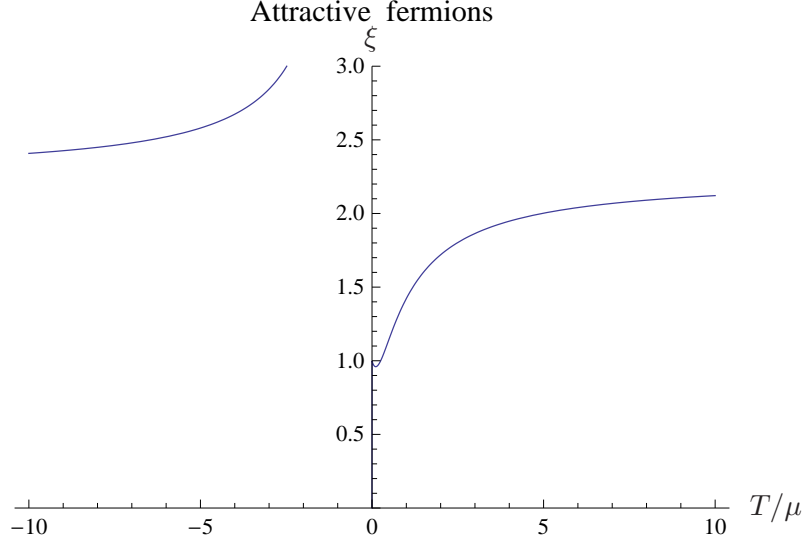


FIG. 8: The energy per particle scaling function ξ for attractive fermions as a function of T/μ .

and

$$\frac{\eta}{s} \approx \frac{\pi}{2\sqrt{2}} (1/(\log(\mu/T) - 2) + T/2\mu) \quad (79)$$

In terms of the density:

$$\lim_{\mu/T \rightarrow \infty} \frac{\eta}{s} = \frac{\pi}{2\sqrt{2} \log(2\pi n/mT)} \quad (80)$$

It is important to note that although the energy per particle scaling function ξ approaches the free field value at low temperatures, the above behavior is very different from the free field case. In the latter, the scaling function $c = -6\text{Li}_2(-z)/\pi^2$, which gives the diverging behavior at very low temperature:

$$\frac{\eta}{s} \approx \frac{3}{4\sqrt{2}\pi} \frac{\mu}{T}, \quad (\text{free fermions}) \quad (81)$$

Finally, as $\mu/T \rightarrow -\infty$, $y \approx 1 + z$, and $c \approx 6z/\pi^2$ and $n \approx mTz/2\pi$. This leads

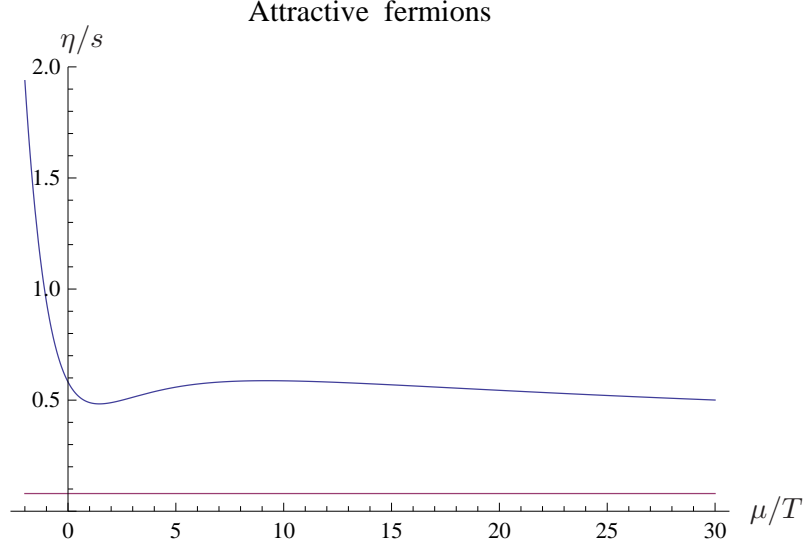


FIG. 9: The ratio η/s as a function of μ/T . The horizontal line is $1/4\pi$.

to exponential growth:

$$\lim_{\mu/T \rightarrow -\infty} \frac{\eta}{s} = -\frac{\pi T}{2\sqrt{2}\mu} e^{-\mu/T} = -\frac{mT}{4\sqrt{2}} \frac{1}{n \log(2\pi n/mT)} \quad (82)$$

VII. ATTRACTIVE BOSONS IN 2 DIMENSIONS

Using the same definitions as for fermions in eq. (51), the integral equation for bosons is

$$y = 1 \pm \frac{2}{y} \log(1 - zy) \quad (83)$$

where the $+$ ($-$) sign refers to repulsive (attractive) interactions. The scaling function c is now

$$c = \frac{6}{\pi^2} \left(\text{Li}_2(zy) + \frac{1}{2}(1 - y^{-1}) \log(1 - zy) \right) \quad (84)$$

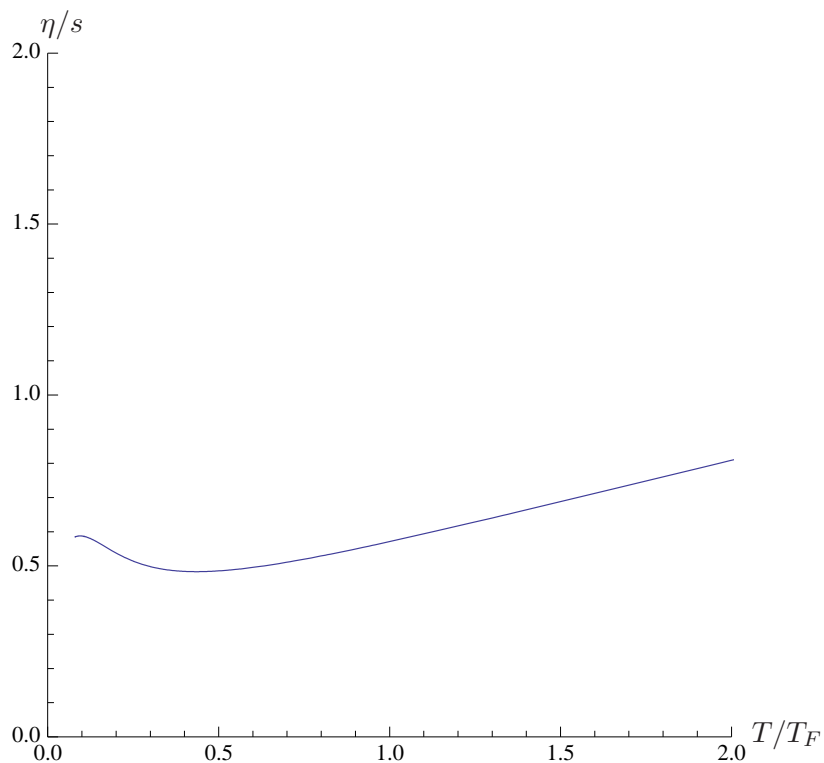


FIG. 10: The ratio η/s as a function of T/T_F for attractive fermions.

The scaling function b has the same expression as in eq. (55), with the above c . The density now is

$$n = -\frac{mT}{2\pi} \log(1 - zy) \quad (85)$$

The energy per particle scaling functions now take the form:

$$\tilde{\xi} = -\frac{2 \log(2)c}{\log(1 - zy)} \quad (86)$$

and

$$\xi = \left(\frac{\log z}{\log(1 - zy)} \right)^2 b \quad (87)$$

For this bosonic case, there is only a solution to eq. (83) for $z \leq z_c \approx .34$, or $\mu/T \leq -1.08$. The density is shown in Figure 13, and note that it has a maximum.

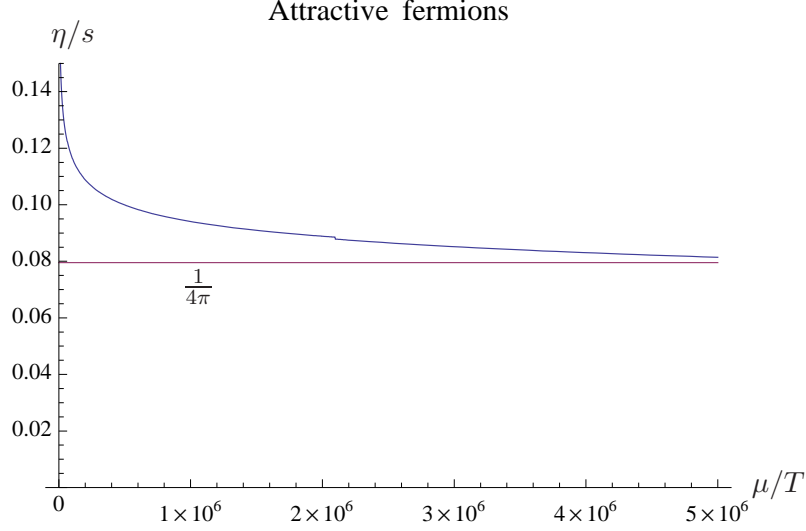


FIG. 11: The ratio η/s as a function of μ/T as μ/T gets very large.. The horizontal line is $1/4\pi$.

The filling fractions are shown for several μ/T up to $\log z_c$. From these plots, it appears that f is diverging at $\mathbf{k} = 0$ as z approaches z_c , suggestive of condensation to a superfluid. Let us refer to the maximum density then as the critical density

$$n_c \approx 1.24 \frac{m k_B T}{2\pi \hbar^2} \iff T_c \approx 0.81 T_F \quad (88)$$

The scaling function c is shown in Figure 15. The limiting value is

$$c(z_c) \approx 0.35 \quad (89)$$

which is considerably less than for a free boson with $c = 1$. The function b decreases to zero at $T/\mu \rightarrow 0$, and the limiting value is

$$b(z_c) \approx 0.94 \quad (90)$$

The energy per particle scaling functions ξ and $\tilde{\xi}$ are shown in Figures 16, 17.

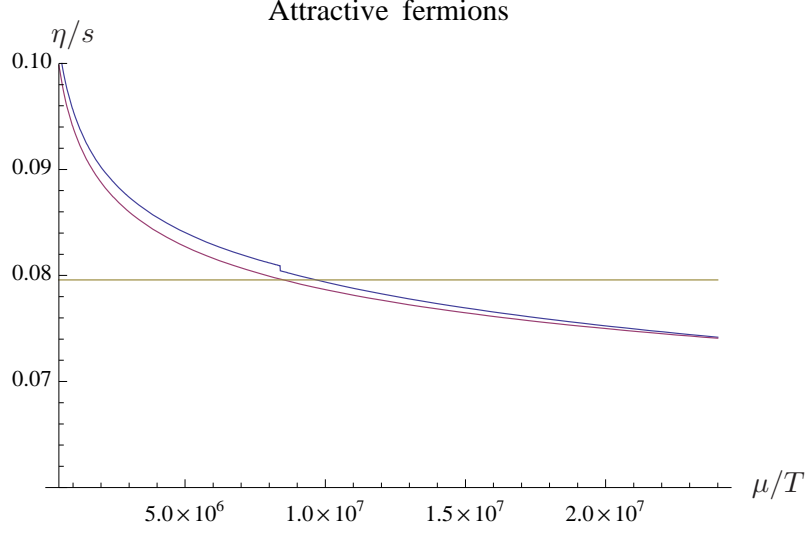


FIG. 12: The ratio η/s as a function of μ/T in the limit of very low temperatures (top curve). The horizontal line is $1/4\pi$. The bottom curve is the approximation eq. (79).

The limiting values are

$$\lim_{\mu/T \rightarrow -\infty} \tilde{\xi} = 0.842766, \quad \tilde{\xi}(z_c) \approx 0.39 \quad (91)$$

and

$$\lim_{T/\mu \rightarrow 0^-} \xi = \infty, \quad \xi(z_c) \approx 2.3 \quad (92)$$

As for the fermionic case, the value $\tilde{\xi} = 0.842766 = 12 \log 2/\pi^2$ implies the energy per particle $\epsilon_1 = T$, which means the gas is in the classical limit.

The ratio η/s given by the expressions eq. (73) with the appropriate bosonic c and b . We find that η/s has its minimum value at z_c , where it is actually below the bound

$$\frac{\eta}{s} \geq 0.4 \frac{\hbar}{4\pi k_B} \quad (93)$$

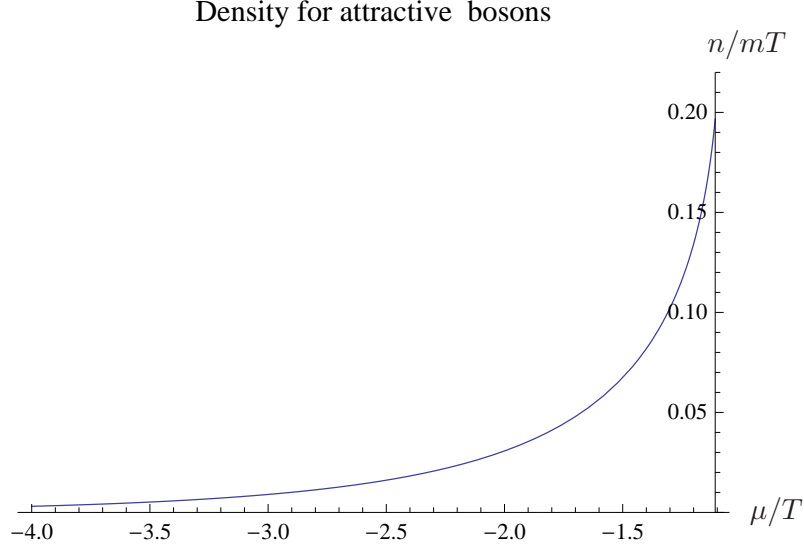


FIG. 13: Density of the attractive bosons as a function of μ/T . The origin of the axes is at $(\log z_c, 0)$.

VIII. REPULSIVE FERMIONS AND BOSONS IN 2 DIMENSIONS

A. Fermions

There are solutions to the eq. (53) for all $\mu/T < 0$, and the density is positive in this range. A plot of the density is shown in Figure 18. The density maximizes at $\mu/T \approx -0.56$, where $n/mT \approx 0.04$. This seems physically reasonable given the strong repulsion in the unitary limit. In contrast, for small coupling g , the kernel $G \approx -g$, and there are solutions for positive chemical potential. In the bosonic case, our formalism leads to a critical density of $n_c = \frac{mT}{2\pi} \log(2\pi/mg)$ for the Kosterlitz-Thouless transition[20]. The filling fractions are shown in Figure 19. Note that they are considerably smaller than in the attractive case, as expected. The scaling

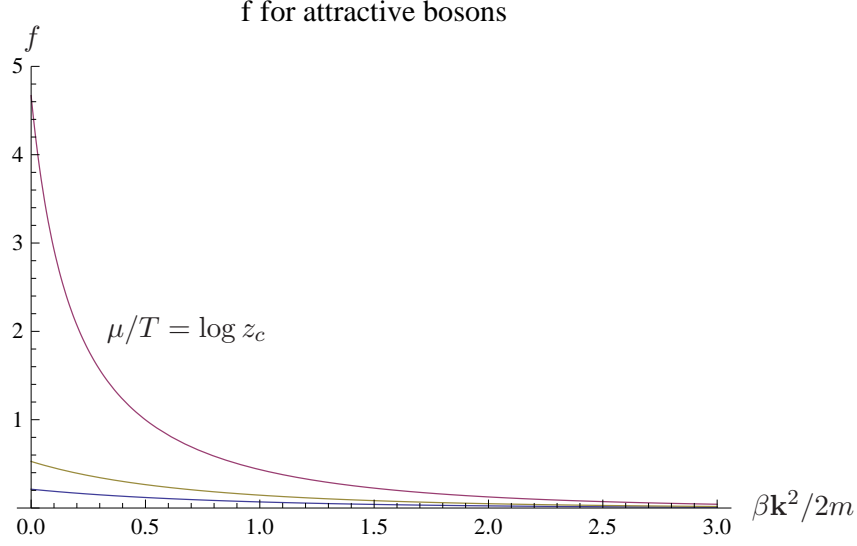


FIG. 14: The filling fraction f for attractive bosons for $\mu/T = -2, -1.5, -1.08 = \log z_c$.

function c is shown in Figure 20. It has the limiting value

$$\lim_{\mu/T \rightarrow 0} c = 0.303964, \quad (94)$$

which is considerably less than the free field value $c = 1/2$. The scaling function b has the limiting values $\lim_{T/\mu \rightarrow 0^-} b = 0$, and $\lim_{T/\mu \rightarrow -\infty} b = \infty$.

Since the pressure is proportional to c , the same density occurs at two different pressures. One sees that for $\mu/T < -0.56$, the density increases with pressure as it should. For $\mu/T > -0.56$ the density decreases with increasing pressure, violating $dp/dV < 0$, and should thus be viewed as an unphysical region. We interpret this as a phase transition occurring at $z_c = e^{-0.56} = 0.57$, where the critical density

$$n_c = 0.25 \frac{mk_B T}{2\pi \hbar^2} \iff T_c \approx 4.0 T_F \quad (95)$$

At this critical point $c(-0.56) = 0.24$. This perhaps corresponds to a transition to a crystalline phase. We cannot prove this, since we have not calculated the shear

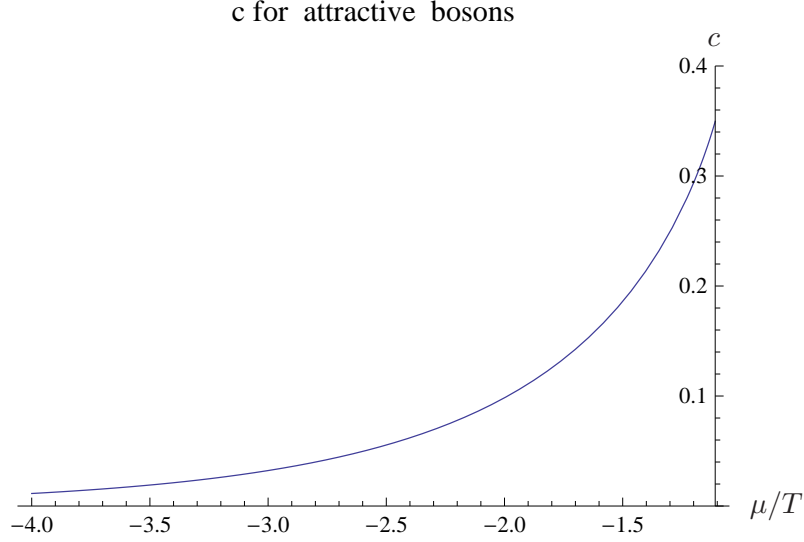


FIG. 15: The scaling function c for attractive bosons as a function of μ/T . The origin of the axes is at $(\log .33, 0)$.

modulus for instance, and it could simply be an artifact of our approximation, but let us take it as a hypothesis. Whereas a Wigner crystal phase occurs at low density in three dimensions, it occurs at high density in two dimensions[33]. The possibility of crystal phases for repulsive bosons was studied in [9]. For Coulomb repulsion with strength e^2 , the thermodynamic state of a classical Coulomb system is determined by $\Gamma = \sqrt{\pi n} e^2 / k_B T$, where n is the density. Experimentally it was found that $\Gamma \approx 137$ [34], which gives a critical density

$$n_c \approx 2.15 \times 10^9 T^2 \frac{1}{\text{cm}^2 K^2} \quad (96)$$

On the other hand, since our model has point-like interactions, and is in the unitary limit, the conditions for a crystal phase are expected to be different. In particular our formula eq. (95) has no e^2 dependence, and this leads to a linear in T dependence.

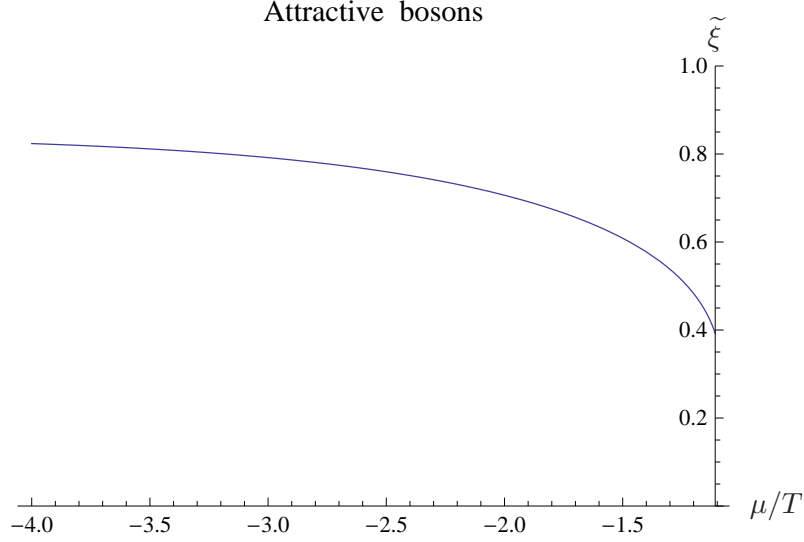


FIG. 16: The energy per particle scaling function $\tilde{\xi}$ for attractive bosons as a function of μ/T .

For m equal to the electron mass

$$n_c \approx 4.5 \times 10^9 T \frac{1}{\text{cm}^2 K} \quad (97)$$

It is interesting to note that for T of order 1, which is where the data in [34] was taken, the two densities (96) and (97) are comparable.

The energy per particle function $\tilde{\xi}$ is shown in Figure 21. The limiting values are:

$$\lim_{\mu/T \rightarrow -\infty} \tilde{\xi} = 0.842766, \quad \tilde{\xi}(z_c) = 1.32 \quad (98)$$

As in previous cases, the above value of $\tilde{\xi}$ implies $\epsilon_1 = T$ as $\mu/T \rightarrow -\infty$ and the gas is thus in the classical limit. Beyond the critical point where the density increases, $\lim_{\mu/T \rightarrow 0} \tilde{\xi} = \infty$. Note that $\tilde{\xi}$ starts to diverge around the proposed phase transition at $\mu/T = -0.56$. Finally the other energy per particle function ξ is less interesting, as it diverges at both endpoints of the density range where the density goes to zero.

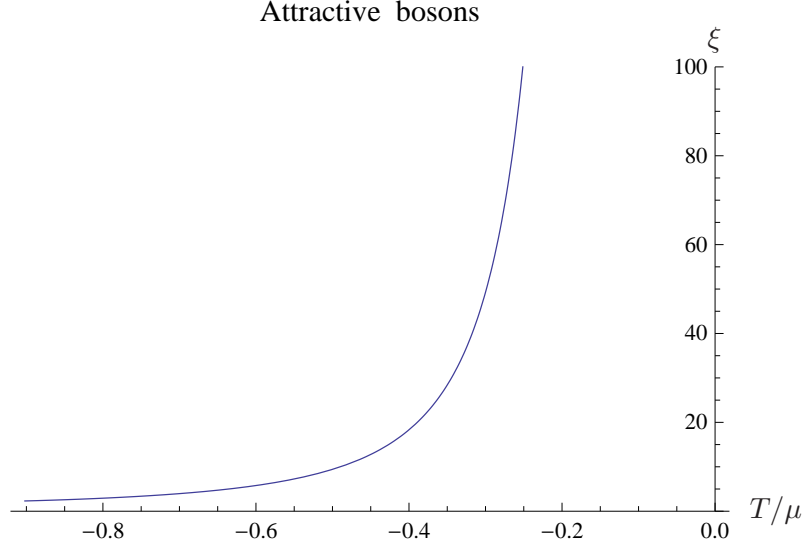


FIG. 17: The energy per particle scaling function ξ for attractive bosons as a function of T/μ .

At the critical point it is still quite large: $\xi(z_c) = 12.6$.

The ratio η/s reaches its minimum near z_c , and is quite large compared to the attractive case:

$$\frac{\eta}{s} \geq 22.6 \frac{\hbar}{4\pi k_B} \quad (99)$$

B. Repulsive Bosons

The repulsive boson case is similar to the repulsive fermion, except that now there are only positive density solutions to the eq. (83) for $\mu/T < -\log 2$. Figure 22 compares the density for bosons versus fermions. The maximum density for bosons, which could again possibly signify a critical point at $z_c \approx e^{-1.45} = 0.235$, is half that

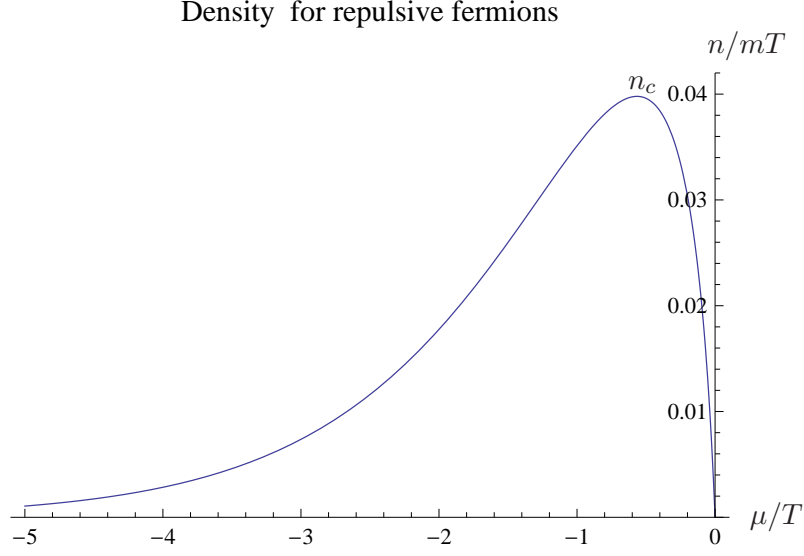


FIG. 18: Density of the repulsive fermionic case as a function of μ/T .

of the fermion case:

$$n_c = 0.125 \frac{mk_B T}{2\pi\hbar^2} \iff T_c \approx 8.0 \epsilon_F \quad (100)$$

At this point $c(-1.3) \approx 0.11$.

The ratio η/s is shown in Figure 23. It has a minimum at $\mu/T = -1.72$ near the critical point and in the physical region:

$$\frac{\eta}{s} \geq 8.85 \frac{\hbar}{4\pi k_B} \quad (101)$$

Recall, the region $\mu/T > -1.45$ is unphysical.

IX. MULTIPLE SPECIES OF PARTICLES

Let us suppose the gas consists of multiple species of particles labeled by the index “a”, of mass m_a , chemical potential μ_a , and statistical parameter $s_a = \pm 1$. Introduce

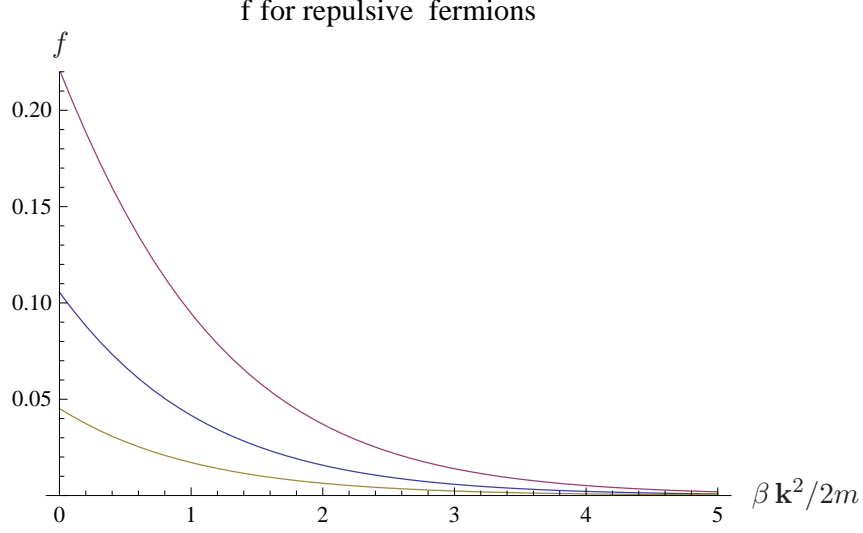


FIG. 19: Filling fraction f for repulsive fermions for $\mu/T = -3, -2, -0.55$. The top curve corresponds to the critical density in eq. (95).

a pseudo-energy $\varepsilon_a(\mathbf{k})$ for each type of particle and the filling fractions:

$$f_a(\mathbf{k}) = \frac{1}{e^{\beta \varepsilon_a(\mathbf{k})} - s_a} \quad (102)$$

As shown in Appendix B, in our approximation, the pseudo-energies satisfy the coupled integral equations:

$$\varepsilon_a(\mathbf{k}) = \omega_a(\mathbf{k}) - \mu_a - \frac{1}{\beta} \log \left(1 + \beta \sum_b G_{ab} * \frac{y_b^{-1}}{e^{\beta \varepsilon_b} - s_b} \right) \quad (103)$$

where $\omega_a(\mathbf{k}) = \mathbf{k}^2/2m_a$,

$$y_a \equiv e^{-\beta \delta_a}, \quad \delta_a \equiv \varepsilon_a - \omega_a + \mu_a \quad (104)$$

and G_{ab} is the 2-body scattering kernel. By Galilean invariance, the kernel is a function of $|v_a - v_b|$ where $v = k/m$ is a velocity. For any function g we defined:

$$(G_{ab} * g)(\mathbf{k}) \equiv \int (d\mathbf{k}') G_{ab}(\mathbf{k}, \mathbf{k}') g(\mathbf{k}') \quad (105)$$

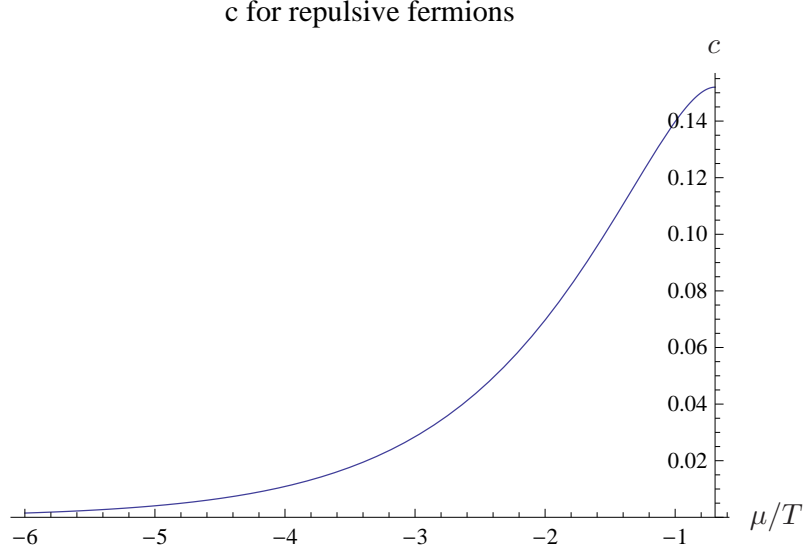


FIG. 20: The scaling function c for repulsive fermions as a function of μ/T .

The free energy density then takes the simple form:

$$\mathcal{F} = -\frac{1}{\beta} \sum_a \int (d\mathbf{k}) \left[-s_a \log(1 - s_a e^{-\beta \varepsilon_a}) - \frac{1 - y_a^{-1}}{2(e^{\beta \varepsilon_a} - s_a)} \right] \quad (106)$$

For the two-component fermion defined by the action (3), spin up particles scatter with spin down, and $G_{\uparrow\downarrow} = G_{\downarrow\uparrow}$. Thus, if the chemical potentials are equal, $\mu_{\uparrow} = \mu_{\downarrow} = \mu$, then $\varepsilon_{\uparrow} = \varepsilon_{\downarrow}$, and the thermodynamics is just two copies of the single component fermion described above. In particular, the density and c are doubled, but the energy per particle scaling functions are the same.

X. CONCLUSIONS

We have shown that the S-matrix based approach to quantum gases developed in [20] leads to a new treatment of the scale-invariant unitary limit, where all of the thermodynamic scaling functions can be computed as a function of μ/T . Though our

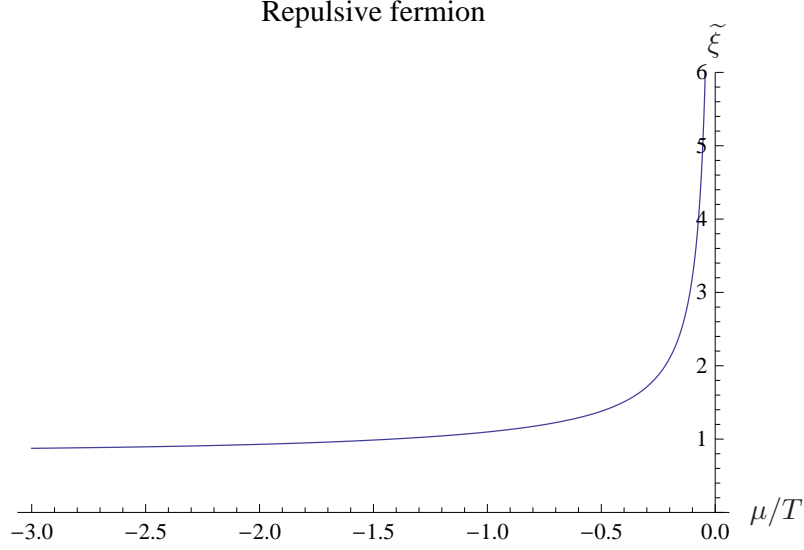


FIG. 21: The energy per particle scaling function $\tilde{\xi}$ for repulsive fermions as a function of μ/T .

methods are of course not exact, they are sufficiently novel to provide new insights into these systems. It would be worthwhile to understand the corrections to our results due to other types of diagrams involving N -body scattering for $N > 2$, and also other more complicated diagrams involving 2-body scattering; this can be systematically explored using the full formalism in [20].

In this paper we have mainly analyzed the 2-dimensional case, deferring the analysis of the integral equations in the 3-dimensional case to a separate publication[23]. For the 2-dimensional case, this required us to define a meaningful unitary limit where the S-matrix equals -1 , and such a limit has not been considered before. We have calculated most of the interesting scaling functions for the free energy and energy per particle.

The ratio of the shear viscosity to entropy density η/s was also analyzed, and for fermions and repulsive bosons, it is above the conjectured lower bound of $\hbar/4\pi k_B$.

Density for repulsive fermions verses bosons

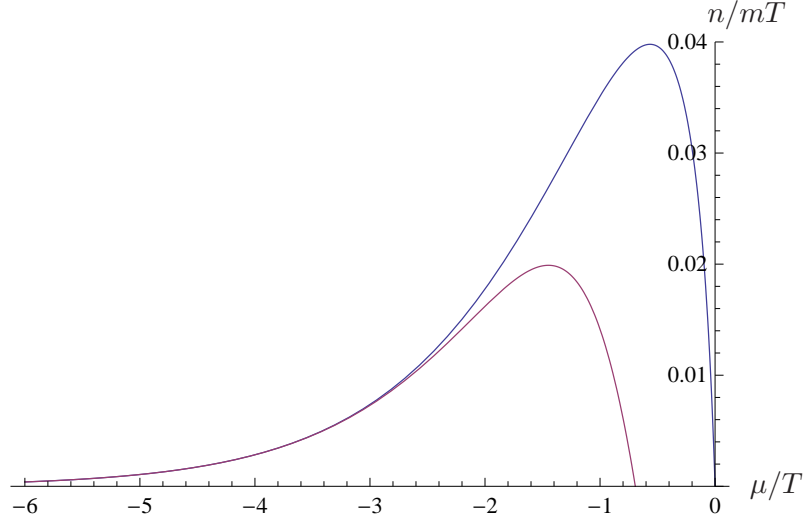


FIG. 22: Density of repulsive bosons (bottom curve) verses fermions as a function of μ/T .

For attractive bosons it drops below it by a factor of 0.4, however this could be an artifact of our approximation. For attractive fermions, the conjectured lower bound is reached at very large $\mu/T \approx 10^7$, however this was argued to occur in an unphysical or metastable region; in the physical regions, $\eta/s \geq 6.07 \hbar/4\pi k_B$.

XI. ACKNOWLEDGMENTS

We thank Erich Mueller for helpful discussions. This work is supported by the National Science Foundation under grant number NSF-PHY-0757868.

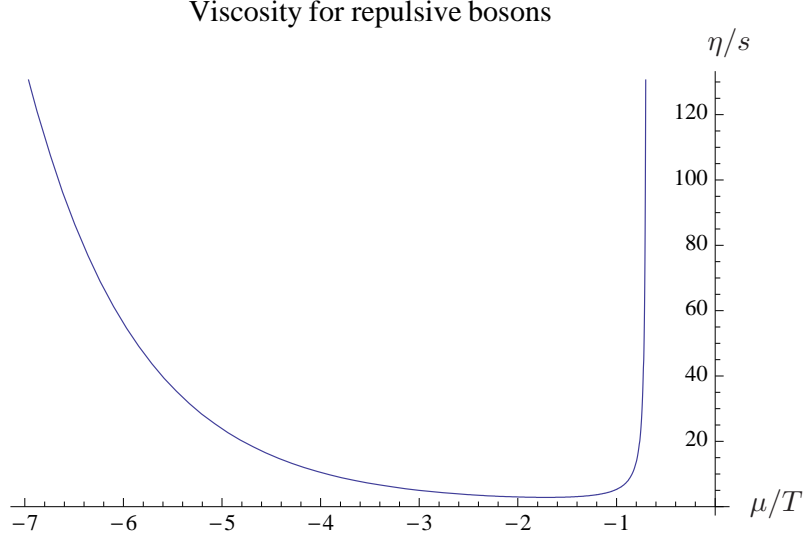


FIG. 23: The ratio η/s as a function of μ/T for repulsive bosons.

XII. APPENDIX A: THE BETA FUNCTION

Consider a single free boson with action eq. (2). Setting the external energy and momentum to zero, the 4-point vertex at tree-level plus 1-loop is

$$\Gamma^{(4)} = -ig - \frac{(-ig)^2}{2} \int \frac{d\omega d^d \mathbf{k}}{(2\pi)^{d+1}} \left(\frac{i}{w - \mathbf{k}^2/2m + i\epsilon} \right) \left(\frac{i}{-\omega - \mathbf{k}^2/2m + i\epsilon} \right) \quad (107)$$

The ω integral can be done by closing the contour in the upper half plane picking up the pole at $\omega = -\mathbf{k}^2/2m + i\epsilon$:

$$1\text{-loop} = -i \frac{mg^2}{2} \int \frac{d^d \mathbf{k}}{(2\pi)^d} \frac{1}{\mathbf{k}^2} \quad (108)$$

Introducing an ultraviolet cut-off Λ :

$$\Gamma^{(4)} = -i \left(g - \frac{mg^2 \Lambda^{d-2}}{\pi^{d/2} \Gamma(d/2) 2^d (d-2)} \right) \quad (109)$$

Defining the dimensionless coupling \widehat{g} as $g = \Lambda^{2-d}\widehat{g}$, and requiring the $\Gamma^{(4)}$ be independent of Λ gives the beta function:

$$\frac{d\widehat{g}}{d\ell} = (2-d)\widehat{g} - \frac{m}{\pi^{d/2}\Gamma(d/2)2^d}\widehat{g}^2 \quad (110)$$

where $\ell = -\log \Lambda$ is the logarithm of a length scale; increasing ℓ corresponds to flowing to lower energy. With the convention for the coupling g in eq. (3) for the fermionic case, the beta-function is the same as above but to half the symmetry factor of the 1-loop diagram.

XIII. APPENDIX B: DERIVATION OF THE MULTI-COMPONENT CASE

In this appendix, we extend the derivation in [20] to the general case of multiple species of particles, of possibly mixed Bose/Fermi statistics. Following the definitions in section VII, the 2-body foam diagram approximation is obtained by considering the free energy functional:

$$F = -\frac{1}{\beta} \int (d\mathbf{k}) \sum_a \left(s_a \log(1 + s_a f_a) - \frac{f_a - f_{0,a}}{1 + s_a f_{0,a}} \right) \quad (111)$$

$$- \frac{1}{2} \int (d\mathbf{k})(d\mathbf{k}') \sum_{a,b} \widetilde{f}_a(\mathbf{k}) G_{ab}(\mathbf{k}, \mathbf{k}') \widetilde{f}_b(\mathbf{k}') \quad (112)$$

where

$$f_{0,a} = \frac{1}{e^{\beta(\omega_a - \mu_a)} - s_a}, \quad \widetilde{f}_a = f_a / y_a \quad (113)$$

The integral equation for the pseudo-energy ε_a follows from the variational principle $\delta F / \delta f_a = 0$. Using

$$\frac{\delta \widetilde{f}_a(\mathbf{k})}{\delta f_b(\mathbf{k}')} = \delta_{a,b} (2\pi)^d \delta(\mathbf{k} - \mathbf{k}') \frac{s_a f_{0,a}}{1 + s_a f_{0,a}}, \quad (114)$$

after some algebra one obtains the integral equation (103). (We have used $G_{ab}(k, k') = G_{ba}(k', k)$.) Using the solution to the integral equation (103) in the

expression for F , one obtains the free energy density $\mathcal{F} = F$ in eq. (106).

-
- [1] K. M. O'Hara et. al., *Science* **298** (2002) 2179.
 - [2] J. Kinast et. al. *Science* **298** (2002) 2179.
 - [3] A. J. Leggett, in *Modern Trends in the Theory of Condensed Matter*, Springer, Berlin 1980.
 - [4] P. Nozières and S. Schmitt-Rink, *J. Low Temp. Phys.* **59** (1985) 195.
 - [5] T.-L. Ho, *Universal Thermodynamics of Degenerate Quantum Gases in the Unitary Limit*, *Phys. Rev. Lett.* **92** (2004) 090402 [arXiv:cond-mat/0309109].
 - [6] T.-L. Ho and E. Mueller, *High temperature expansion applied to fermions near a Feshbach resonance*, *Phys.Rev.Lett.* **92** (2004) 160404 [arXiv:cond-mat/0306187].
 - [7] Y. Ohashi and A. Griffin, *The BCS-BEC Crossover in a Gas of Fermi Atoms with a Feshbach Resonance*, *Phys. Rev. Lett.* **89** (2002) 130402 [arXiv:cond-mat/0210185].
 - [8] Astrakharchik, J. Boronat, J. Casulleras and S. Giorgini, *Equation of state of a Fermi gas in the BEC-BCS crossover: a quantum Monte Carlo study*, *Phys. Rev. Lett.* **93** (2004) 200404 [arXiv:cond-mat/0406113].
 - [9] E. B. Kolomeisky and J. P. Straley, *Renormalization-group analysis of the ground-state properties of dilute bose systems in d spatial dimenions*, *Phys. Rev.* **B46** (1992) 11749.
 - [10] Z. Nussinov and S. Nussinov, *The BCS-BEC Crossover in Arbitrary Dimensions*, [arXiv:cond-mat/0609106].
 - [11] A. Bulgac, J. E. Drut and P. Magierski, *Spin 1/2 Fermions in the Unitary Regime: A Superfluid of a New Type*, *Phys. Rev. Lett.* **96** (2006) 090404 [arXiv:cond-mat/050537].
 - [12] D. Lee, *Ground state energy of spin 1/2 fermions in the unitary limit*, *Phys. Rev.* **B73** (2006) 115112 [arXiv:cond-mat/0511332].

- [13] E. Burovski, N. Prokof'ev, B. Svistunov and M. Troyer, *The Fermi-Hubbard model at unitarity*, New J.Phys.**8** (2006) 153 [arXiv:cond-mat/0605350]; *Critical Temperature and Thermodynamics of Attractive Fermions at Unitarity*, Phys. Rev. Lett. **96** (2006) 160402.
- [14] Y. Nishida and D. T. Son, ϵ expansion for a Fermi gas at infinite scattering length, Phys. Rev. Lett. **97** (2006) 050403 [arXiv:cond-mat/0604500].
- [15] P. Nikolić and S. Sachdev, *Renormalization group fixed points, universal phase diagram, and $1/N$ expansion for quantum liquids with interactions near the unitarity limit*, Phys. Rev. **A75** (2007) 033608 [arXiv:cond-mat/0609106].
- [16] D. T. Son, *Toward an AdS/cold atoms correspondence: a geometric realization of the Schoedinger symmetry*, Phys. Rev. **D78** (2008) 046003 [arXiv:0804.3972].
- [17] J. Maldacena, D. Martelli and Y. Tachikawa, *Comments on string theory backgrounds with non-relativistic conformal symmetry*, JHEP0810 (2008) 072 [arXiv:0807.1100].
- [18] C. P. Herzog, M. Rangamani and S. F. Ross, *Heating up Galilean holography*, JHEP0811 (2008) 080 [arXiv:0807.1099].
- [19] A. Adams, K. Balasubramanian and J. McGreevy, *Hot spacetimes for cold atoms*, JHEP0811:059, 2008 [arXiv:0807.1111].
- [20] P.-T. How and A. LeClair, *Critical point of the two-dimensional Bose gas: an S-matrix approach*, Nucl. Phys. **B824** (2010) 415 [arXiv:0906.0333].
- [21] E. Lieb and W. Liniger, Phys. Rev. **130** (1963) 1605.
- [22] C. N. Yang and C. P. Yang, Jour. Math. Phys. **10**, (1969) 1115.
- [23] P.-T. How and A. LeClair, *S-matrix approach to quantum gases in the unitary limit II: the three-dimensional case*, in preparation.
- [24] P. Kovtun, D. T. Son and A. O. Starinets, Phys. Rev. Lett. **94** (2005) 111606 [arXiv:hep-th/0405231].
- [25] D. S. Petrov, M. A. Baranov and G. V. Shlyapnikov, *Superfluid transition in quasi 2d*

- Fermi gases*, Phys. Rev. **A 67** (2003) 031601 [arXiv:cond-mat/02112061].
- [26] E. Kapit and A. LeClair, *A model of a 2d non-Fermi liquid with $SO(5)$ symmetry, AF order, and a d-wave SC gap*, J. Phys. **A42** (2009) 025402 [arXiv:0805.4182].
- [27] A. LeClair, *Interacting Bose and Fermi gases in low dimensions and the Riemann hypothesis*, Int. J. Mod. Phys. **A23** (2008) 1371 [arXiv:math-ph/0611043].
- [28] F. Reif, *Fundamentals of statistical and thermal physics*, McGraw-Hill 1965.
- [29] P. Massignan, G. M. Bruun and H. Smith, *Viscous relaxation and collective oscillations in a trapped Fermi gas near the unitarity limit*, Phys. Rev. **A71** (2005) 033607 [arXiv:cond-mat/0409660].
- [30] B. A. Gelman, E. V. Shuryak and I. Zahed, *Cold Strongly Coupled Atoms Make a Near-perfect Liquid*, Phys. Rev. **A72** (2005) 043601 [arXiv:nucl-th/0410067].
- [31] T. Schäfer, *The Shear Viscosity to Entropy Density Ratio of Trapped Fermions in the Unitarity Limit*, Phys. Rev. **A76** (2007) 063618 [arXiv:cond-mat/0701251].
- [32] G. Rupak and T. Schafer, *Shear viscosity of a superfluid Fermi gas in the unitarity limit*, Phys. Rev. **A76** (2007) 073607 [arXiv:0707.1520].
- [33] R. S. Crandall and R. Williams, Phys. Lett. **34A** (1971) 404.
- [34] C. C. Grimes and G. Adams, *Evidence for a Liquid-to-Crystal Phase Transition in a Classical, Two-Dimensional Sheet of Electrons*, Phys. Rev. Lett. **42** (1979) 795.